



OPEN ACCESS

RECEIVED
12 October 2020REVISED
14 December 2020ACCEPTED FOR PUBLICATION
3 January 2021PUBLISHED
15 January 2021



Original content from
this work may be used
under the terms of the
[Creative Commons
Attribution 4.0 licence](#).

Any further distribution
of this work must
maintain attribution to
the author(s) and the title
of the work, journal
citation and DOI.



LETTER

Observation of strong magneto plasmonic nonlinearity in bilayer graphene discs

Matthew L Chin^{1,2}, Sebastian Matschy³, Florian Stawitzki³, Jayaprakash Poojali¹, Hassan A Hafez⁴, Dmitry Turchinovich⁴, Stephan Winnerl⁵, Gagan Kumar⁶, Rachael L Myers-Ward⁷, Matthew T Dejarld⁷, Kevin M Daniels¹, H Dennis Drew¹, Thomas E Murphy¹  and Martin Mittendorff³ 

¹ University of Maryland, College Park, MD 20740, United States of America

² U.S. Army Research Laboratory, Adelphi, MD 20783, United States of America

³ Universität Duisburg-Essen, Duisburg 47057, Germany

⁴ Universität Bielefeld, Bielefeld 33615, Germany

⁵ Helmholtz-Zentrum Dresden-Rossendorf, Dresden 01328, Germany

⁶ Indian Institute of Technology Guwahati, Guwahati, Assam 781039, India

⁷ U.S. Naval Research Laboratory, Washington D.C. 20375, United States of America

E-mail: matthew.l.chin2.civ@mail.mil

Keywords: graphene plasmonics, THz pump-probe, magneto plasmons, tunable nonlinearity, THz nonlinearity

Abstract

Graphene patterned into plasmonic structures like ribbons or discs strongly increases the linear and nonlinear optical interaction at resonance. The nonlinear optical response is governed by hot carriers, leading to a red-shift of the plasmon frequency. In magnetic fields, the plasmon hybridizes with the cyclotron resonance, resulting in a splitting of the plasmonic absorption into two branches. Here we present how this splitting can be exploited to tune the nonlinear optical response of graphene discs. In the absence of a magnetic field, a strong pump-induced increase in on-resonant transmission can be observed, but fields in the range of 3 T can change the characteristics completely, leading to an inverted nonlinearity. A two temperature model is provided that describes the observed behavior well.

1. Introduction

For the past decade, graphene, a two-dimensional (2D) allotrope of carbon, has been studied extensively. As a Dirac semimetal described by a linear dispersion relation, graphene possesses a novel band structure where charge carriers act as effectively massless fermions, which has led to a number of special unique properties, including its record-high carrier mobility [1], high thermal conductivity [2], flat broadband absorption of 2.3% per monolayer [3], tunable carrier density, as well as strong terahertz (THz) plasmons [4–9]. With uncharacteristically strong light–matter interactions across both the infrared and THz frequency ranges, graphene is a promising candidate material for optoelectronic and plasmonic devices [10–14]. The collective oscillations of charge carriers in graphene are distinctly different from the plasmonic response of noble metals. In addition to possessing different dispersion relations, 2D plasmons in graphene are typically active in the THz and far-IR spectrum range rather than the visible and near-IR spectrum range of metals. The carrier density (and in consequence, the effective doping) of graphene can also be tuned through electrostatic gating, leading to a modification of the plasmonic resonance frequency [4, 7, 10, 15]. Similar to their noble metal counterparts, periodic structures in graphene are accompanied with orders-of-magnitude increase in the radiation absorption at the plasmon frequency and localized field enhancement in their immediate vicinity. Finally, externally applied magnetic fields can be used to tune the plasmonic resonance frequency of graphene [16–18]. This is due to graphene's small effective cyclotron mass, and thus, the graphene's cyclotron frequency being comparable to the plasmon frequency. It has been shown experimentally that the magneto-optical response can be enhanced due to the generation of graphene magnetoplasmons [19].

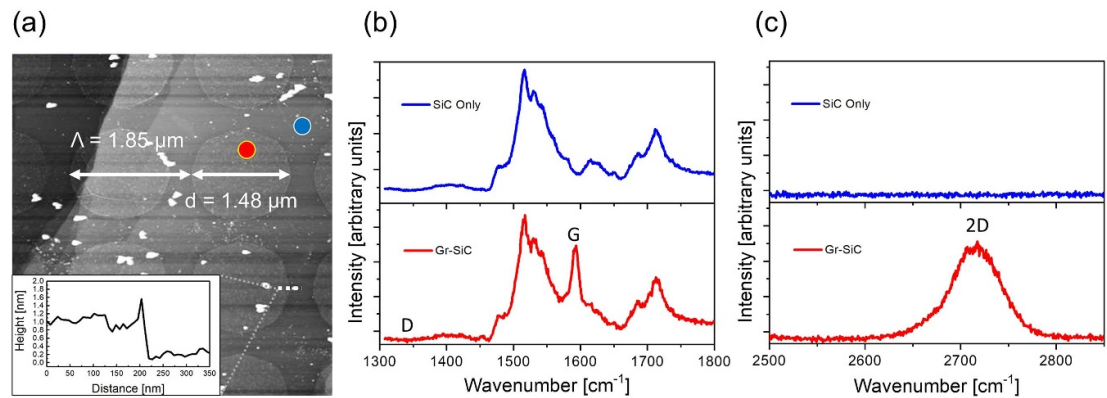


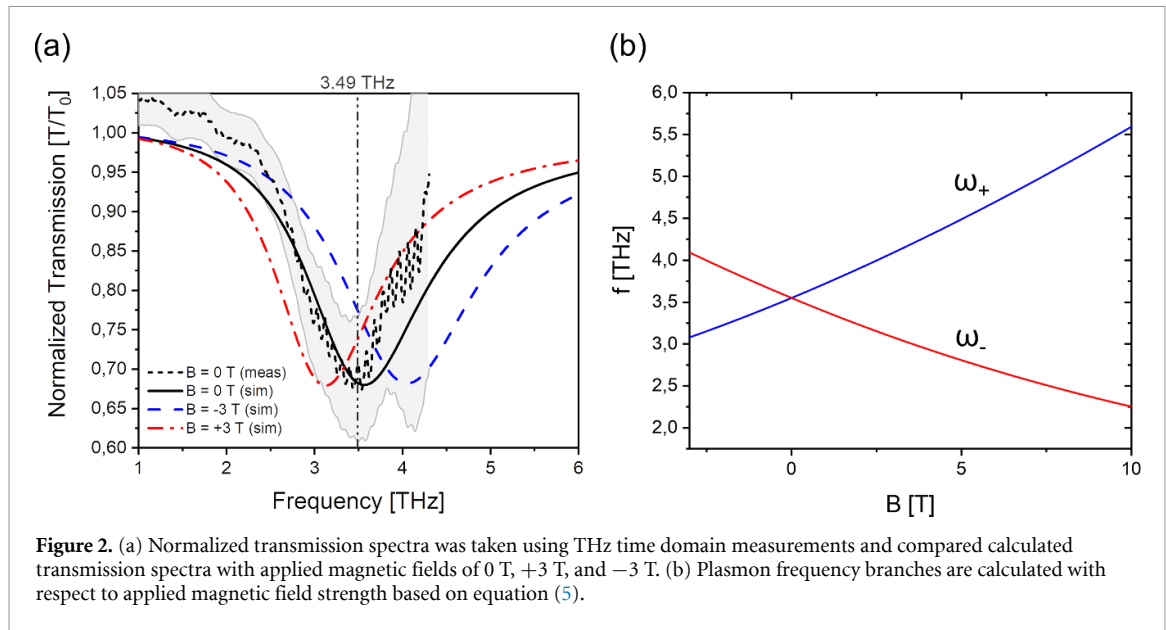
Figure 1. (a) Atomic force microscopy image of fabricated bilayer graphene disc array on SiC is shown, with the inset showing the height profile of the dotted line across the SiC-graphene step. (b) Raman spectra of bilayer graphene grown on SiC is compared with a bare SiC substrate. The presence of a G peak at $\sim 1590\text{ cm}^{-1}$ and the lack of a D peak at $\sim 1350\text{ cm}^{-1}$ indicates the presence of low-defect graphene as presented in previous literature [31, 32]. (c) Additionally, Raman spectra taken between 2500 cm^{-1} and 2850 cm^{-1} wavenumber shows the existence of a broad 2D peak at $\sim 2720\text{ cm}^{-1}$ that can be characterized by multiple Lorentzian components, with slight bias near 2680 cm^{-1} . This provides strong evidence for the presence of bilayer graphene rather than the expected single Lorentzian peak of monolayer graphene closer to $\sim 2740\text{ cm}^{-1}$ as observed by Röhl *et al* [32].

This combination of tunability of graphene's plasmonic resonance frequency using both electrostatic gating, to dynamically change its carrier density, and an applied magnetic field, to change the cyclotron frequency, has been observed experimentally in the linear response of graphene at THz frequencies. The nonlinear response of graphene at THz frequencies also is significantly enhanced in graphene plasmonic structures [20–22]. This strong nonlinearity is not related to a nonlinear susceptibility in graphene, but dominated by thermal effects in highly doped graphene and can actually be a lot stronger than nonlinear effects directly related to the bandstructure [23, 24]: as the charge carriers are heated by the absorbed THz radiation, the Fermi edge gets smeared out. As the density of states in graphene increases linearly with the energy, the chemical potential has to decrease in order to keep the number of electrons constant. While in most materials thermal nonlinearities are very slow, the carrier cooling in graphene is fast enough to allow for extremely efficient harmonic generation in the THz range [25]. The same effect leads to an ultrafast red shift of the plasmon frequency in graphene plasmonic structures, resulting in pump-induced increase of the transmission on the order of 10% at moderate pump fluence [26, 27]. Here we study the tunability of this strong thermal nonlinearity in patterned, SiC-sublimated bilayer graphene discs in the presence of magnetic fields. Using THz pump-probe spectroscopy we found that the nonlinear response can be dramatically altered in moderate magnetic fields, leading even to an inversion of the nonlinear response at fields as low as 3 T.

2. Fabrication and characterization

Graphene was grown on SiC using the SiC sublimation process on the Si-face of the wafer at a temperature of $1050\text{ }^{\circ}\text{C}$ in a carrier gas mixture of hydrogen and argon. A hydrogen passivation technique was used to create a quasi-freestanding bilayer graphene film, reducing the effects associated with substrate coupling [28–30]. The graphene was patterned into a $2\text{ mm} \times 2\text{ mm}$ square array of discs with diameters of $1.48\text{ }\mu\text{m}$ and with a periodicity of $1.85\text{ }\mu\text{m}$ using electron-beam lithography. A polymethyl methacrylate (PMMA) resist was used as a mask for the oxygen plasma etch to remove the exposed graphene, thereby forming isolated discs. After the etch, the resist was removed using heated acetone. Figure 1(a) provides an atomic force micrograph showing the patterned graphene discs and the periodicity. Raman spectroscopy based on a 532 nm laser line was used to confirm the existence and quality of the graphene. In figure 1(b), the G peak is located at the expected location of $\sim 1580\text{ cm}^{-1}$, and the 2D peak appears to possess the broader, up-shifted shape and slight shoulder between $\sim 2650\text{ cm}^{-1}$ and $\sim 2750\text{ cm}^{-1}$ that is characteristic of bilayer graphene [31, 32].

Prior to the nonlinear measurements, we used conventional THz time-domain spectroscopy to measure the plasmon resonance of the discs in the absence of a magnetic field. A bare SiC chip served as reference, the measurements were done at room temperature in a nitrogen purged environment to suppress water absorption. The measured transmission as a function of the frequency is plotted in figure 2(a): when the frequency is resonant with the plasmon frequency at around 3.5 THz , a peak extinction of about 30% is observed. This matches well with calculations via the electromagnetic field simulation software CST Studio Suite with the simulated transmission spectra also shown in figure 2(a). The graphene discs were modeled by prescribing a magnetic field-dependent dielectric tensor matrix based on the Drude conductivity equations [33]



$$\sigma_{xx}(\omega, B) = \frac{q^2 |E_F|}{\pi \hbar^2} \frac{\gamma - i\omega}{(\gamma - i\omega)^2 + \omega_c^2(B)} \quad (1)$$

$$\sigma_{xy}(\omega, B) = -\frac{q^2 |E_F|}{\pi \hbar^2} \frac{\omega_c(B)}{(\gamma - i\omega)^2 + \omega_c^2(B)} \quad (2)$$

where tensor components are described by the graphene Fermi energy, E_F , carrier charge, q , reduced Planck's constant, \hbar , and the carrier scattering rate of the graphene, γ . The magnetic field dependence was incorporated through the addition of a cyclotron frequency, ω_c , where the cyclotron frequency can be expressed as the transition energy E_c of the highest occupied and the lowest unoccupied Landau level via $\omega_c = E_c/\hbar$ with \hbar as the reduced Planck constant. Since the graphene discs consist of AB stacked bilayer graphene, the Landau level energy equation [34, 35]

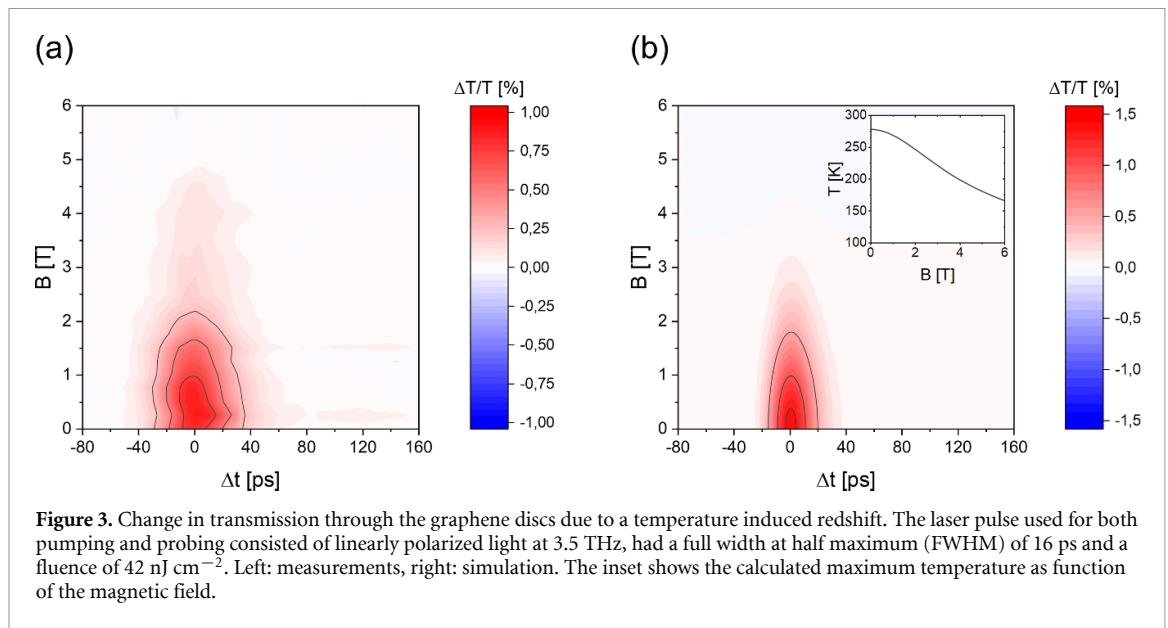
$$E_n = \frac{1}{\sqrt{2}} \left[\gamma_1^2 + (2n+1) \Delta_B^2 - \sqrt{\gamma_1^4 + 4(2n+1) \gamma_1^2 \Delta_B^2 + \Delta_B^4} \right]^{\frac{1}{2}}, \quad (3)$$

with $\Delta_B = \sqrt{2\hbar|qB|}v_F$, B as the externally applied magnetic field normal to the graphene, v_F as the Fermi velocity of graphene, n as the Landau level index and γ_1 as the interlayer hopping term, was used to calculate the energy of the involved Landau levels. For the interlayer hopping term a value of $\gamma_1 = 0.3$ eV led to good results in the simulation; the value is also in excellent agreement with measurements done in other works [36–38]. The cyclotron energy $E_c = E_{n+1} - E_n$ depends on the Fermi energy and the applied magnetic field. Compared to single layer graphene, where the cyclotron frequency can be more easily calculated via $\omega_c = ev_F^2 B/|E_F|$, the cyclotron frequency is slightly increased, leading to a more pronounced splitting: the cyclotron energy is about 4.2 meV at 3 T and increases roughly linearly to about 14 meV at 10 T. This behavior, which deviates strongly from the Landau-level energy that increases with the square root of the magnetic field, is only observed in highly doped graphene, where the Fermi energy is far above the cyclotron energy [39] ($E_F \approx 320$ meV for our sample).

The simulated normalized transmission using incident left-handed circularly polarized radiation provides the expected frequency shift of the peak extinction due to the change in the external magnetic field. Figure 2(a) provides the simulated linear response for applied magnetic fields of 0 T, 3 T, and −3 T, and compares them to the measured linear response from THz time domain measurements. Applying a magnetic field of ± 3 T induces a splitting between the right- and left-circular plasmon resonances that is comparable to the plasmon linewidth.

3. Pump-probe measurements and two-temperature model

To characterize the nonlinear absorption of the magneto plasmons, we performed pump-probe measurements at the free-electron laser (FEL) facility FELBE at the Helmholtz-Zentrum



Dresden-Rossendorf. FELBE provides THz pulses with a duration in the picosecond range and a repetition rate of 13 MHz. The photon frequency is tunable in a wide range, which allows for measurements above and below the resonance. The first set of measurements were performed at a photon frequency of about 3.5 THz, which is nearly resonant with the room-temperature plasmon frequency of the discs. FELBE naturally provides linearly polarized radiation. Quarter-wave plates, made of quartz, were used to convert the linearly polarized radiation to circular polarized radiation independently for pump and probe radiation. The FEL pulses had a duration of 16 ps and 20 ps for the linear and circular polarization, respectively. A second set of measurements were performed significantly above resonance at 4.3 THz with linearly polarized radiation (and a 6.4 ps pulse duration). A pellicle beam sampler was used to split off about 2% of the radiation to serve as the probe and was guided through a mechanical delay stage to vary the time delay between the pump and probe pulses. A parabolic mirror was used to focus the parallel pump and probe beams under a small angle to the sample that was kept in a magneto-optical cryostat at a temperature of 60 K in a helium atmosphere. Magnetic fields of up to $\pm 7 \text{ T}$ were applied perpendicular to the sample (i.e. normal to the bilayer graphene discs). The transmitted probe radiation was collected after passing through the magneto-optical cryostat using a second parabolic mirror and guided to a bolometer while the residual pump radiation was spatially filtered out. The pump-induced change in transmission was then recorded as a function of the time delay between the pump and probe beam.

A set of pump-probe measurements taken with linearly polarized radiation and magnetic fields of up to 6 T is shown in figure 3(a). The relative change in transmission at a pump fluence of 42 nJ cm^{-2} is color coded as a function of the time delay (horizontal axis) and the magnetic field (vertical axis). Without magnetic field, a pump-induced increase in transmission of about 0.8% was observed, which is consistent with measurements on graphene ribbons made from the same material [21]. Within about 40 ps, the signal relaxes back to equilibrium, as the hot carriers cool to the lattice. The increase in transmission is attributed to the redshift of the plasmon frequency as the hot carrier distribution results in a decreased chemical potential. For fields above 1 T, the pump-probe signal is strongly suppressed, until above 5 T where the signal could no longer be observed.

In order to understand the physical background of the vanishing signal, we performed numerical modeling of the pump-probe experiment. The model is based on the two-temperature model that was already exploited to investigate the nonlinear absorption of graphene plasmonic ribbons in the absence of a magnetic field [21, 26]. The absorption as a function of the frequency was calculated via

$$\frac{\Delta T(\omega)}{T_0} = \left| 1 + \frac{dZ_0}{\pi(1+n_{\text{SiC}})} \frac{D(T)}{\left(\Gamma(T) - i \frac{\omega^2 - \omega_p^2(T)}{\omega} \right)} \right|^{-2}, \quad (4)$$

where d represents the fraction of the surface covered by graphene, Z_0 is the free space impedance, and n_{SiC} is the refractive index of the SiC substrate. The Drude weight D , scattering rate Γ , and plasmon frequency ω_p

depend on the temperature of the carrier distribution (for details see [21]). To account for the magnetic field, the plasmon frequency in equation (1) was replaced by [16]

$$\omega_{\pm} = \sqrt{\frac{\omega_c^2}{4} + \omega_p} \pm \frac{|\omega_c|}{2}. \quad (5)$$

To derive the temperature evolution of the free carriers during the pump-probe cycles, the differential equation [40–42]

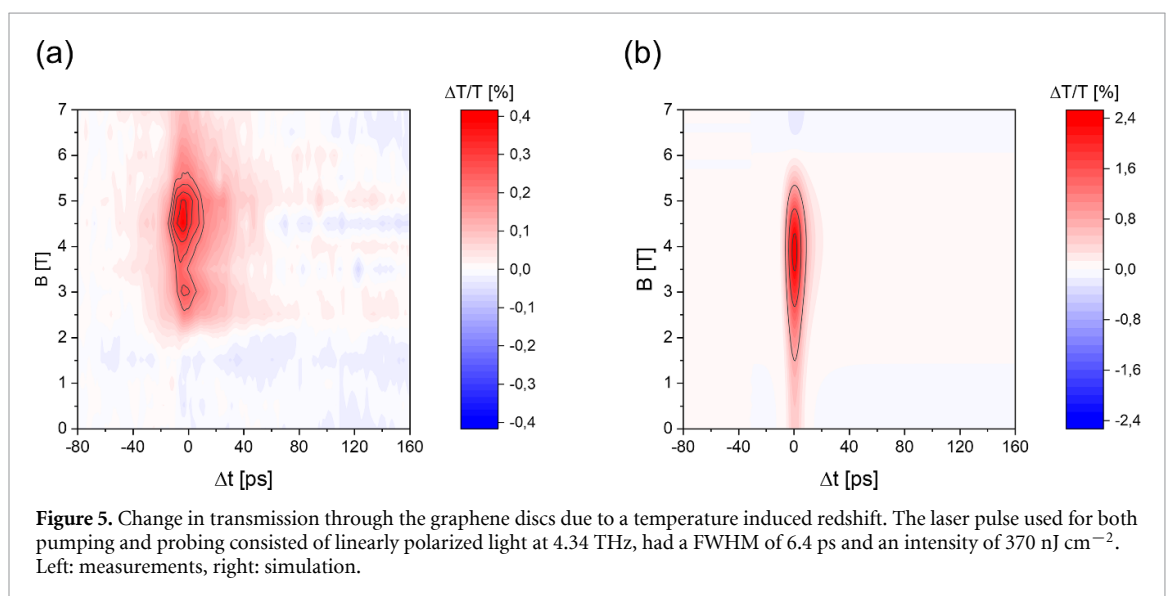
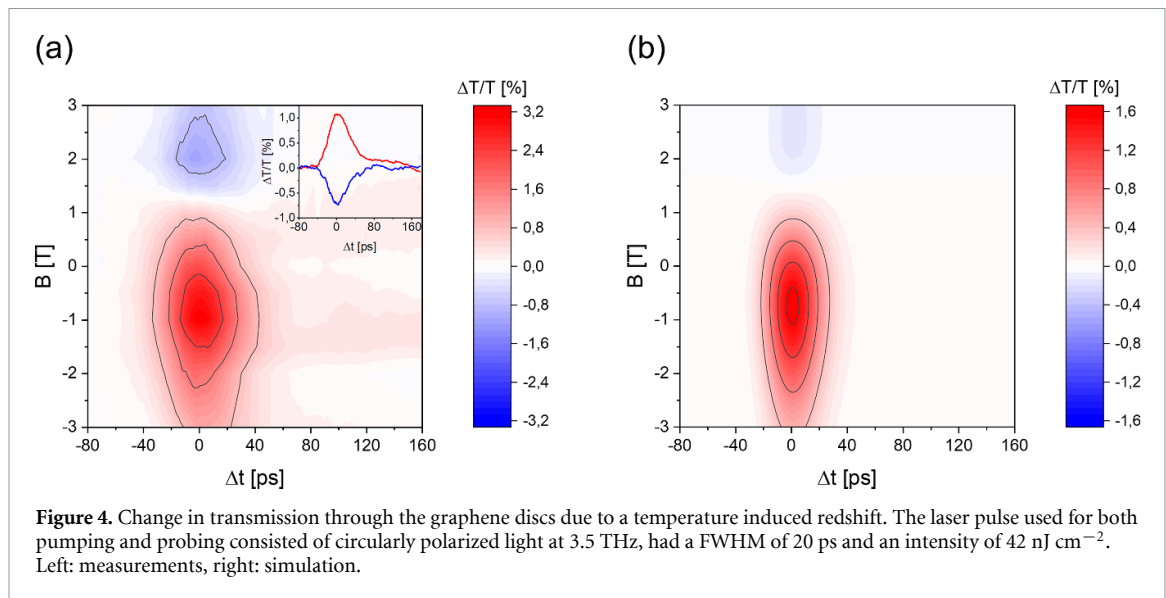
$$\alpha T \frac{dT}{dt} + \beta (T^3 - T_L^3) = A(\omega, T) I(t), \quad (6)$$

with α as the specific heat of the electron gas, T_L as the lattice temperature and A as the absorption coefficient, was used. The laser intensity $I(t)$ describes the temporal evolution of the pump pulse, which is assumed to be Gaussian, the pulse duration was derived from the measured FEL spectra. Further parameters for the model are a Fermi energy E_F of 320 meV, a plasmon frequency ω_p of $2\pi \cdot 3.55$ THz as well as a constant scattering rate Γ of $2\pi \cdot 0.8$ THz. For the supercollision cooling coefficient β , a value of $1 \text{ W m}^{-2} \text{ K}^{-3}$ was chosen to fit the relaxation time in the model to the experimental data; the value is also in good agreement with values reported in previous works [40, 41].

As can be seen in figure 3(b), the results of the model match well with the experimental data. Interestingly, the model shows significant heating of the carrier distribution even at high magnetic fields, where no pump-probe response is measured (see inset in figure 3(b)). This is caused by the red shift of the plasmon frequency upon carrier heating, which results in a pump-induced increase (decrease) in transmission when the photon frequency is above (below) the plasmon frequency. As the magnetic field is applied and the plasmon frequency splits up into the upper and the lower branch, the linearly polarized radiation interacts with both branches. While the lower branch leads to an increase of the transmission, the upper branch causes the transmission to decrease, leading to no net change of the transmission above 5 T.

To further investigate the role of the upper and the lower branch, we performed pump-probe measurements with circularly polarized pump and probe radiation. In this case, only one of the two branches is interacting with the pump and probe radiation. For the measurements taken using linearly polarized radiation, the orientation of the magnetic field does not play a role, but for measurements using circularly polarized radiation, the sign of the magnetic field actually determines which of the two branches interacts with the radiation. The results of this experiment, in which the magnetic field was tuned in the range between -3 T and 3 T are shown in figure 4(a). A positive change in transmission is observed at -3 T, indicating that the plasmon frequency is below the photon frequency. As the magnetic field is tuned towards zero, the amplitude of the pump-probe signal increases, until resonance is reached at about -0.8 T and the maximum increase in transmission is observed. For increasing positive magnetic fields, the signal reduces to zero and eventually changes sign above 1.5 T. The negative sign of the signals can again be understood by the thermal redshift of the plasmon frequency caused by the hot carriers. As was the case for linearly polarized radiation, the calculations match the experimental findings for the circularly polarized qualitatively, though the absolute values are less well matched. Note, that no fitting parameter is included to match the signal strength to the measurements. Furthermore, the two-temperature model does not account for variations of the scattering rate between the upper and the lower branch, which might be present due to the different character of the electron motion: the higher frequency mode corresponds to circular electron motion within the discs while the lower frequency mode is associated with skipping orbits on the edge. This distinction becomes stronger for high fields. Additionally, it does not account for the experimental conditions, that might not be perfect for all measurements.

To investigate the detuning of the magneto plasmons, the FEL was significantly detuned with respect to the plasmon frequency. At a wavelength of $69 \mu\text{m}$ (4.34 THz), no pump-probe signal was observed without a magnetic field present. As the measurement was performed with linearly polarized radiation, only one orientation of the magnetic field was measured. For elevated fields of more than 2 T, a clear positive pump-probe signal is observable, the peak change in transmission is around 4.5 T, and at 7 T, only a slight change in transmission is measurable (see figure 5(a)). This evolution of the peak change in transmission with respect to magnetic field is expected as the magneto plasmon is tuned into resonance with the photon frequency at around 4 T. For magnetic fields below that value, the magneto plasmon frequency is below the photon frequency, leading to positive, but small pump-induced changes in transmission. Above 5 T, the magneto plasmon frequency is above the photon frequency and a sharp drop in signal is expected, eventually leading to a change in sign at maximum fields as shown in the calculation in figure 5(b). In comparison to the measurements shown in figures 3 and 4, the signal is shorter, which is mostly caused by the shorter pulse duration of the FEL, which is around 6.4 ps at this frequency compared to 20 ps in the earlier measurements.



This shorter pulse duration has been taken into account in the model as well, with the results being shown in figure 5(b). Unlike previous studies on unpatterned graphene that reported an increase in relaxation time in strong magnetic fields [39, 43], only a slight dependence on the magnetic field was observed. Without a magnetic field, a relaxation time of 21 ps was observed at resonance, which increased to 27 ps at 4.5 T. This might be related to the bilayer nature of the sample, or defects enabling scattering with out-of-plane phonons [44].

4. Conclusion

In conclusion, we investigated the influence of a magnetic field to the optical nonlinearity observed in graphene plasmons. Depending on the relative photon frequency with respect to the plasmon frequency, the nonlinear behavior can be tuned in a wide range, i.e. the pump-induced increase in transmission at resonance can be inverted to a pump-induced decrease with moderate magnetic fields in the 3 T range. In contrast to earlier experiments on multilayer epitaxial graphene, only a minor change in relaxation time was observed. A two temperature model provides a good description of the experiment.

Acknowledgments

Funded by the Deutsche Forschungsgemeinschaft (DFG, German Research Foundation)—Project-ID 278162697—SFB 1242. We thank J Michael Klopff and the ELBE team for assistance.

ORCID iDs

Thomas E Murphy  <https://orcid.org/0000-0002-8286-3832>

Martin Mittendorff  <https://orcid.org/0000-0003-3998-2518>

References

- [1] Morozov S V, Novoselov K S, Katsnelson M I, Schedin F, Elias D C, Jaszczak J A and Geim A K 2008 *Phys. Rev. Lett.* **100** 016602
- [2] Ghosh S, Calizo I, Teweldebrhan D, Pokatilov E P, Nika D L, Balandin A A, Bao W, Miao F and Lau C N 2008 *Appl. Phys. Lett.* **92** 151911
- [3] Nair R R, Blake P, Grigorenko A N, Novoselov K S, Booth T J, Stauber T, Peres N M R and Geim A K 2008 *Science* **320** 1308
- [4] Ju L *et al* 2011 *Nat. Nanotechnol.* **6** 630
- [5] Koppens F H L, Chang D E and García de Abajo F J 2011 *Nano Lett.* **11** 3370
- [6] Fei Z *et al* 2011 *Nano Lett.* **11** 4701
- [7] Grigorenko A N, Polini M and Novoselov K S 2012 *Nat. Photon.* **6** 749
- [8] Chen J *et al* 2012 *Nature* **487** 77
- [9] Yan H, Xia F, Li Z and Avouris P 2012 *New J. Phys.* **14** 125001
- [10] Yan H, Li X, Chandra B, Tulevski G, Wu Y, Freitag M, Zhu W, Avouris P and Xia F 2012 *Nat. Nanotechnol.* **7** 330
- [11] Otsuji T, Popov V and Ryzhii V 2014 *J. Phys. D: Appl. Phys.* **47** 094006
- [12] Low T and Avouris P 2014 *ACS Nano* **8** 1086
- [13] Cai X, Sushkov A B, Jadidi M M, Nyakiti L O, Myers-Ward R L, Gaskill D K, Murphy T E, Fuhrer M S and Drew H D 2015 *Nano Lett.* **15** 4295
- [14] Bandurin D A *et al* 2018 *Nat. Commun.* **9** 5392
- [15] Poumirol J-M, Liu P Q, Slipchenko T M, Nikitin A Y, Martin-Moreno L, Faist J and Kuzmenko A B 2017 *Nat. Commun.* **8** 14626
- [16] Yan H, Li Z, Li X, Zhu W, Avouris P and Xia F 2012 *Nano Lett.* **12** 3766
- [17] Crassee I, Orlita M, Potemski M, Walter A L, Ostler M, Seyller T H, Gaponenko I, Chen J and Kuzmenko A B 2012 *Nano Lett.* **12** 2470
- [18] Tymchenko M, Nikitin A Y and Martin-Moreno L 2013 *ACS Nano* **7** 9780
- [19] Tamagnone M *et al* 2018 *Phys. Rev. B* **97** 241410
- [20] Gullans M, Chang D E, Koppens F H L, García de Abajo F J and Lukin M D 2013 *Phys. Rev. Lett.* **111** 247401
- [21] Jadidi M M, Daniels K M, Myers-Ward R L, Gaskill D K, König-Otto J C, Winnerl S, Sushkov A B, Drew H D, Murphy T E and Mittendorff M 2019 *ACS Photonics* **6** 302
- [22] Ooi Kelvin J A and Tan Dawn T H 2017 *Proc. R. Soc. A* **473** 20170433
- [23] Hendry E, Hale P J, Moger J, Savchenko A K and Mikhailov S A 2010 *Phys. Rev. Lett.* **105** 097401
- [24] Hipolito F, Taghizadeh A and Pedersen T G 2018 *Phys. Rev. B* **98** 205420
- [25] Hafez H A *et al* 2018 *Nature* **561** 507
- [26] Jadidi M M, König-Otto J C, Winnerl S, Sushkov A B, Drew H D, Murphy T E and Mittendorff M 2016 *Nano Lett.* **16** 2734
- [27] Cox J D and García de Abajo F J 2019 *Nano Lett.* **19** 3743
- [28] Riedl C, Coletti C, Iwasaki T, Zakharov A A and Starke U 2009 *Phys. Rev. Lett.* **103** 246804
- [29] Emery J D, Wheeler V D, Johns J E, McBriarty M E, Detlefs B, Hersam M C, Kurt Gaskill D and Bedzyk M J 2014 *Appl. Phys. Lett.* **105** 161602
- [30] Daniels K M, Jadidi M M, Sushkov A B, Nath A, Boyd A K, Sridhara K, Drew H D, Murphy T E, Myers-Ward R L and Gaskill D K 2017 *2D Mater.* **4** 025034
- [31] Ferrari A C *et al* 2006 *Phys. Rev. Lett.* **97** 187401
- [32] Röhl J, Hundhausen M, Emtsev K V, Seyller T H, Graupner R and Ley L 2008 *Appl. Phys. Lett.* **92** 201918
- [33] Bludov Y V, Ferreira A, Peres N M R and Vasilevskiy M I 2013 *Int. J. Mod. Phys. B* **27** 1341001
- [34] Milton Pereira J Jr Peeters F M and Vasilopoulos P 2007 *Phys. Rev. B* **76** 115419
- [35] Yuan S, Roldán R and Katsnelson M I 2011 *Phys. Rev. B* **84** 125455
- [36] Malard L M, Nilsson J, Elias D C, Brant J C, Plentz F, Alves E S, Castro Neto A H and Pimenta M A 2007 *Phys. Rev. B* **76** 201401(R)
- [37] Zhang L M, Li Z Q, Basov D N and Fogler M M 2008 *Phys. Rev. B* **78** 235408
- [38] McCann E and Koshino M 2013 *Rep. Prog. Phys.* **76** 056503
- [39] Mittendorff M, Orlita M, Potemski M, Berger C, de Heer W A, Schneider H, Helm M and Winnerl S 2014 *New J. Phys.* **16** 123021
- [40] Graham M W, Shi S-F, Ralph D C, Park J and McEuen P L 2013 *Nat. Phys.* **9** 103–8
- [41] Graham M W, Shi S-F, Wang Z, Ralph D C, Park J and McEuen P L 2013 *Nano Lett.* **13** 11
- [42] Song J C W, Reizer M Y and Levitov L S 2012 *Phys. Rev. Lett.* **109** 106602
- [43] Plochocka P, Kossacki P, Golnik A, Kazimierzczuk T, Berger C, de Heer W A and Potemski M 2009 *Phys. Rev. B* **80** 245415
- [44] Wendler F *et al* 2017 *Phys. Rev. Lett.* **119** 067405